International Journal of Concrete Structures and Materials
Vol.11, No.1, pp.45–58, March 2017
DOI 10.1007/s40069-016-0183-2
ISSN 1976-0485 / eISSN 2234-1315

Preliminary Structural Design of Wall-Frame Systems for Optimum Torsional Response

George K. Georgoussis*

(Received March 12, 2016, Accepted November 20, 2016, Published online December 27, 2016)

Abstract: Recent investigations have pointed out that current code provisions specifying that the stiffness of reinforced concrete elements is strength independent, and therefore can be estimated prior to any strength assignment, is incorrect. A strength allocation strategy, suitable for preliminary structural design of medium height wall-frame dual systems, is presented for allocating strength in such buildings and estimating the dependable rigidities. The design process may be implemented by either the approximate continuous approach or the stiffness matrix method. It is based on the concept of the inelastic equivalent single-degree-of-freedom system which, the last few years, has been used to implement the performance based seismic design. The aforesaid strategy may also be used to determine structural configurations of minimum rotation distortion. It is shown that when the location of the modal centre of rigidity, as described in author's recent papers, is within a close distance from the mass axis the torsional response is mitigated. The methodology is illustrated in ten story building configurations, whose torsional response is examined under the ground motion of Kobe 1995, component KJM000.

Keywords: earthquake engineering, inelastic structures, strength dependent stiffness, asymmetric buildings, modal center of rigidity.

1. Introduction

Force-based methods for seismic design, as recommended by current building codes, have been questioned during the last two decades, in the sense that the selection of a more or less arbitrary force reduction (behavior) factor may not lead to a safer design, as potential damage is related more on the deformation capacity of the structure rather than on its strength. In more explicit terms, the concept that multistory buildings may be designed on the basis of a single force-reduction factor, depending on the structural type and not on the structural geometry (Priestley et al. 2007; Priestley 2000) is lacking in that the deformation capacity of the system under a horizontal loading is unknown and hence its vulnerability to seismic actions. As stated by Priestley (2000), two different buildings designed to the same code and with the same force-reduction or ductility factors may experience different levels of damage under a given earthquake. In other words, a proper design should be based on the principle that the seismic demand (the deformations induced by the seismic excitations) should be matched with the capacity of the structure to sustain such deformations. This approach, generally termed as 'performance-based design', is recommended the last few years to complement the current seismic design philosophy (Chopra and Goel 1999, 2000; Fajfar 2000; Heo and Kunnath 2013). Two major strategies are adopted by this approach: at first, based on experimental evidence, it became clear that because of the inelastic behavior of structural members and the associated ductility property, the magnitude of the induced inertia forces may be much lower than that predicted by an elastic analysis. The second refers to the realization that it is not the level of the design base shear the key point of a structural design, but the distribution of strength among the various members of a given structure, according to the capacity design concept, as it was developed in the seventies by Park and Paulay (1975).

For a well-detailed structure, an inelastic step by step time-history analysis is probably the most realistic procedure to evaluate its seismic response. With this methodology, the elastic or inelastic deformation state of response is taken into account at every step of the analysis, but, evidently, such a method is much more complex than a static procedure, costly and time consuming for structural applications. Besides, it requires an ensemble of representative ground motions to receive reliable information about the response of a given structure. In a few words, it is not practical for every day design use. As a compromise, the pushover analysis has been recommended to provide an estimate of the deformation capacity of structures exposed to seismic actions. In general terms, this procedure, which is the backbone of the 'performance-based design', consists an incremental static analysis under a monotonically increasing static loading

Department of Civil Engineering, School of Pedagogical and Technological Education (ASPETE), 14121 Attica, Greece.
*Corresponding Author; E-mail: ggeorgo@tee.gr

until the top of the structure reaches the target displacement. This is usually bounded by predetermined limits of story drifts (critical for non-structural members) or strains capacities (critical for structural members), or when the base shear—top deflection diagram (pushover curve) drops by more (say) than 20% and the building model is considered unstable further on. This procedure requires that the structural model is well defined: at first a strength assignment of the various members should be implemented. Usually the lateral loading recommended by the code is used to determine yield moments at the locations of potential plastic hinges. The second requirement is that the moment-rotation relationships at these critical sections should also be well defined to allow for plastic deformation when the building is displaced beyond the elastic limits. Having defined the structural model, the inelastic static procedure, under increasing lateral loads, can easily be performed. A key point of this analysis is the shape of the distributed lateral loading, which, ideally, should represent the deflection profile of the system when it is stressed well into the post-elastic phase. Most of the proposals recommend this procedure for buildings which respond mainly in the translational mode and therefore the pushover analysis can be performed on the symmetrical counterpart of the real building. Three-dimensional pushover analyses performed on plan-asymmetric multi-story buildings have shown that seismic demands at or near the flexible edge are higher due to torsional effects (Moghadam and Tso 2000) and in another paper (Fajfar et al. 2005) it is suggested that the results obtained from the 3D pushover analysis should be combined with those of a linear dynamic analysis in order to assess the torsional amplifications. In fact, modern codes require special precautions for such cases (e.g. EC8 2004, clause 4.3.3.4.2.7).

The pushover curve, thus obtained is then expressed into an idealized bilinear force–displacement relationship (capacity curve) of an equivalent SDOF system (Chopra and Goel 1999, 2000; Fajfar 2000). Both branches of the later curve are drawn by engineering judgment and the slope of the initial branch specifies the 'elastic' period of the equivalent SDOF system, together with its yield displacement. The seismic displacement demand can then be determined from the acceleration design spectrum, when it is transformed in an acceleration–displacement (A–D) format (demand diagram).

When the pushover analysis is used for the evaluation of the seismic performance of existing structures (e.g. EC8-part 3, A3.2.4), it requires a detailed definition of the element stiffnesses, based on the real structural properties (reinforcement detailing, concrete strength, etc.), but this is not the case when it is used for newly designed buildings. The main drawback of this methodology now, is that the pushover curve is drawn on the basis that the element stiffnesses are assumed strength independent, equal to a constant proportion of the gross section stiffness, regardless of the reinforcement content. However, extensive research the last 20 years has demonstrated that the yield curvature of R.C. members is practically a function of the member cross-section depth and steel yield strain and insensitive of the amount of the longitudinal reinforcement. In extensive research conducted in New Zealand (e.g. Paulay 2002, 2003; Priestley and Kowalsky 1998; Priestley 2000; Priestley et al. 2007) it has been found that for wall and column sections, the yield curvatures may be calculated as

$$\Phi_{cy} = k_c \varepsilon_y / d_c \quad \text{for rectangular columns} \tag{1a}$$

$$\Phi_{wy} = k_w \varepsilon_y / d_w \quad \text{for walls} \tag{1b}$$

while for beams, the yield curvature may be taken as

$$\Phi_{by} = k_b \varepsilon_y / d_b \tag{1c}$$

where ε_y is the steel yield strain, d_c, d_w and d_b are the depths of the column, wall and beam sections respectively and the shown coefficients, with an error of $\pm 10\%$, may be approximated with the values of 2.12 (for k_c), 1.8–2.0 (for K_w, depending on the reinforcement details) and 1.7 (for K_b). Therefore, the flexural stiffness of such members, defined by the ratio of the bending moment capacity (which is more or less proportional to the steel content and affected by the presence of the axial load) to the yield curvature is, in fact, strength dependent. As a consequence, the stiffness of any structural member cannot be determined by the size of its lateral cross section, unless its required strength is specified. This means that a reliable pushover curve (and the relevant capacity curve of the equivalent SDOF system) cannot be based on assumed flexural rigidities of member's cracked sections, prior to an estimate of their bending moment capacities.

This paper presents a simple procedure, suitable for preliminary structural design of low to medium height wall-frame dual systems. This type of structures has considerable merits in withstanding seismic actions and it is recommended by some modern codes (e.g. EAK 2000). The formation of the undesirable soft story mechanism is prevented and dual building systems combine the advantages of the two constituent sub-systems: wall and frame (Paulay and Priestley 1992; Garcia et al. 2010). The first objective of the paper is concerned with the assessment of the element flexural strengths and their dependable flexural rigidities, when the building is designed to form a beam-sway plastic mechanism into the inelastic phase. In particular, it is examined whether with this procedure the 'elastic' characteristics of the equivalent SDOF system (frequency and yield displacement or yield acceleration) may be accurately assessed from the first mode data of the elastic structure having the aforementioned rigidities. It is worth reminding here that the current forced-based design procedure of low or medium height structures is practically based on the first mode frequency and on a more or less arbitrary reduction factor. In most of the codes this frequency may be taken as that of the symmetrical counterpart structure and it is calculated on the grounds of flexural rigidities equal to a fraction of member's gross sections.

In Sect. 2, expressions are provided for element flexural strengths and their dependable flexural rigidities, when the building is designed to be displaced as a beam-sway mechanism. In Sect. 3 the limits of inelastic displacements are investigated with respect to the code provisions and member plastic rotation capacities and predictions are made about the onset of yielding. In Sect. 4, it is shown how quick estimates of the 'elastic' characteristics of the equivalent SDOF system can be made by using the approximate continuum approach methodology. More accurate assessments of the 'elastic' characteristics of the equivalent SDOF system can also be made from the first mode data of the elastic discrete multistory system (with flexural rigidities as described in Sect. 2) when it is analyzed by the traditional stiffness method and in the numerical example presented at the end of this paper it is notable the closeness of these values with those provided by the capacity curve of the SDOF system.

The second objective of the paper refers to the torsional behavior of inelastic asymmetric structures. The design procedure described above refers to buildings responding in a more or less translational mode, and the pushover analysis demonstrates the displacement capacity of planar structures. It is generally accepted that eccentricity in buildings is the main cause of the rotational response during strong ground motions, and that in many cases this response may lead to partial or total collapse. In recent years a number of investigations have been carried out to demonstrate the seismic vulnerability of these buildings and qualitative papers have been published from time to time on this issue (e.g. Chandler et al.1996; Paulay 1998, 2001; Rutenberg 1998; De Stefano and Pintucchi 2008; De Stefano et al. 2015; Anagnostopoulos et al. 2015a, b; Bosco et al. 2015; Kyrkos and Anagnostopoulos 2011a, b, 2013). The recognition of the seismic vulnerability of such buildings has also raised the issue of mitigating the torsional effects during a strong ground motion. Most of the studies are based on systems with elements having the traditional strength independent stiffness, but a few of them involve systems with wall elements in which the stiffness is strength dependant (e.g.: Aziminejad et al. 2008; Aziminejad and Moghadam 2009). This issue has also been the subject of author's recent research (Georgoussis 2008, 2009, 2010, 2012, 2014, 2015) in multistory systems with traditional strength independent element stiffnesses. It has been demonstrated that the seismic behavior of linear systems (composed by different types of bents: walls, frames, coupled wall assemblies, etc.) can be accurately assessed by analyzing two simpler systems: (i) the corresponding uncoupled multi-story structure which provides the first mode frequency and effective mass, M_e^*, and (ii) a torsionally coupled equivalent single story system, which has a mass equal to M_e^*, and is supported by elements with stiffnesses equal to the product of $M_e^*$with the squared frequencies of the corresponding real bents (element frequencies) of the assumed multi-story structure. In the case of uniform structures composed by very dissimilar bents, a higher accuracy of the aforementioned analysis can be attained with the use of the effective element frequencies, (Georgoussis 2014). The stiffness centre of the equivalent single story system constitutes the modal centre of rigidity (m-CR) and when this point lies on (or close to) the axis passing through the centers of floor masses, the rotational response sustained by an elastic asymmetric building system is minimum (Georgoussis 2009, 2010, 2012, 2014, 2015). In Sect. 5, the procedure of constructing a structural configuration of minimum torsional response is demonstrated by means of the formulation of the approximate continuous approach, using the strength dependent flexural rigidities of Sect. 2. This is a direct procedure, since the effective element frequencies of walls and frames are given by simple formulae and therefore the location of the stiffness center (m-CR) of the equivalent single story system is easily assessed. The same quantities can also be obtained by the familiar to designers stiffness method and this is demonstrated in the ten story model building examined in Sect. 6.

The third objective of the paper is to demonstrate that the elastic response of minimum torsion is preserved into the inelastic region when the element strength assignment is 'compatible' with static analyses under a lateral loading simulating the first mode of vibration. This has already been shown in asymmetric buildings with traditional, strength independent element rigidities (Georgoussis 2012, 2014, 2015) and can be explained as follows: when a medium or low height building structure, in the linear phase, is responding in a practically translational mode, the effective seismic forces developed are basically proportional to the first translational mode of vibration. Therefore, a strength assignment obtained from a planar static analysis under a set of lateral loads simulating the aforesaid mode of vibration, represents a system in which all potential plastic hinges at the critical sections are formed at about the same time. The almost concurrent yielding of these elements preserves the translational response, attained at the end of the elastic phase, to the post elastic one. This procedure of constructing a structural configuration of minimum rotational response is now investigated in asymmetric systems with elements having strength dependent stiffnesses and this is demonstrated in a ten story eccentric dual building under the ground motion of Kobe 1995, component KJM000.

2. Preliminary Design Considerations

Traditionally, given the configuration layout of a low or medium height building structure, as it has been decided by architectural, esthetic or functional norms, the practicing engineer starts the structural design by estimating the design (base) shear, V_d, required by code provisions. This horizontal force, which is specified as a fraction of the total dead (and portions of live) load W, in relation to a first period dependant coefficient β, as follows:

$$V_d = \beta W \tag{2a}$$

can also be seen as a first estimate of the yield force of an equivalent inelastic SDOF system. The characteristics of this system (mass, frequency, yield displacement) are derived by the following considerations:

As stated in the previous section, the equivalent SDOF system is constructed by assuming first that the real building (Fig. 1a) is subjected to an increasing lateral loading vector, proportional to MΦ (i.e.: V = αMΦ), where M is the mass matrix and Φ is the assumed mode (vector) of deformation (among the various deflection profiles shown in the mentioned figure, Φ is selected to represent a shape of deformation reflecting an advanced inelastic stage). This inelastic static analysis is ended when story drift limits (critical for non-structural members) or strains capacities (critical for structural members) are reached. The base shear—top deflection curve, $V - \Delta$, obtained from this analysis (Fig. 1c) may be approximated by a bilinear curve (shown in the same figure by the dotted line, where the peak load is denoted with V_{do} and the corresponding top displacement with Δ_y) and then it is transformed into the capacity curve, *A-u* (Fig. 1d) by using the following formulation:

$$A = V/M_e^* \quad \text{and} \quad u = \Delta/\Gamma\Phi_r \tag{2b}$$

where M_e^*, u represent the effective (modal) mass and displacement respectively of the SDOF system shown in Fig. 1b. The first of these quantities is given as

$$M_e^* = (\Phi^T \mathbf{M1})^2/\Phi^T \mathbf{M}\Phi \tag{2c}$$

and, in the second of Eq. (2b), Φ_r is the value of the assumed vector Φ at the top (roof) of the structure and, Γ is the (modal) participation factor equal to

$$\Gamma = \Phi^T \mathbf{M1}/\Phi^T \mathbf{M}\Phi \tag{2d}$$

where 1 is the unit vector. The diagram shown in Fig. 1d may be interpreted as the normalized force -displacement relationship of the elasto-plastic SDOF system shown in Fig. 1b, which yields when it is pushed by a static force equal to V_{do}. This force is, in general, higher than the design shear, V_d, and constitutes the over-strength of the structure. There are many possible sources for this reserve strength: effects of gravity loads, order in which the various plastic hinges are formed, redistribution of internal forces, etc. (Humar and Rahgozar 1996). With a proper strength assignment through the structure, as it is described further below, the yield force, V_{do}, may be close to V_d, but in any case the horizontal acceleration causing yield of the SDOF system will be equal to

$$A_y = V_{do}/M_e^* \tag{2e}$$

The yield acceleration, A_y, and the corresponding yield deformation, u_y, are also shown in Fig. 1d, together with the slope of the initial elastic branch, ω_e^2, which represents the square value of the effective frequency.

The procedure described above presumes an estimate of V_d and more importantly a distribution of strength through the building to assess bending moment capacities and flexural rigidities of the various members. However, as strength and stiffness are interrelated, the designer has a considerable choice to allocate strengths in a rather arbitrary way, say according to his experience, with the only restriction being that the limits (on deflections, crack widths, etc.) imposed by the code in the serviceability limit state, where member rigidities are based on lightly cracked sections (under bending moments well below the yield values), should be satisfied. With these considerations, it may be decided, prior to any calculations, just by engineering judgment, what proportion of the design shear V_d (say $V_{df} = \lambda V_d$) is to be resisted by the frame sub-system, and the rest of it, $V_{dw} = (1-\lambda)V_d$, by the wall sub-system. Typical values of λ vary between 0.3 and 0.4, as modern codes (e.g. EC8 2004) define the wall-equivalent dual system as that where the shear resistance of walls exceeds 50% of the total resistance of the building. It is reminded here, that elastic analyses have demonstrated (Paulay and Priestley 1992) that the wall shear in the upper stories is opposite in sense to the external load shear and, as a result, the frame shear exceeds the external shear in these stories. The overall frame shear profile presents little variation from the base to the top of the structure and this means that the allocated frame shear, $V_{df} = \lambda V_d$, may be considered constant over the height of the frame

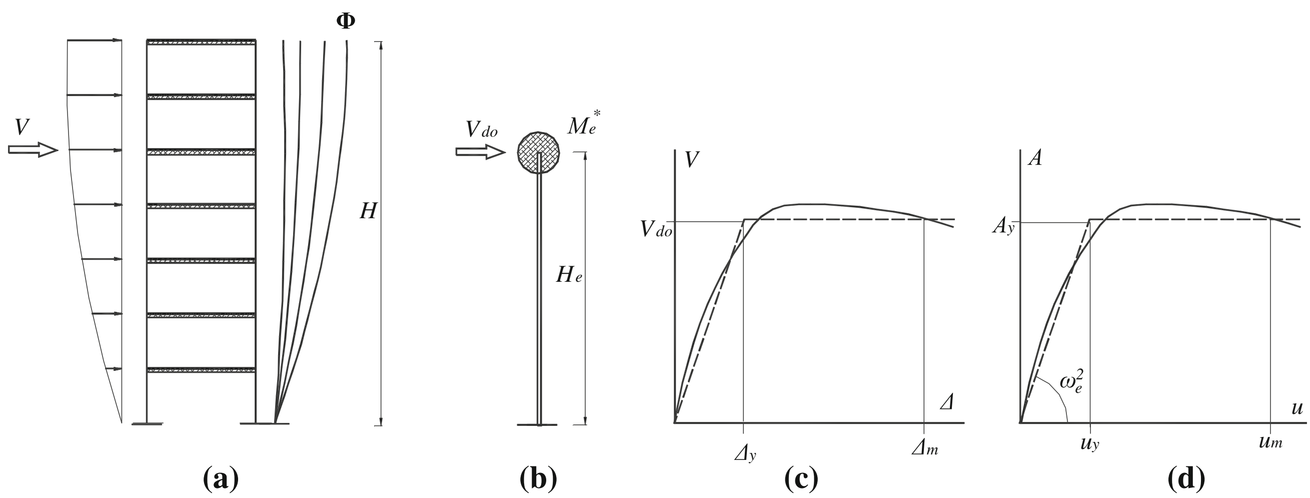

Fig. 1 Constructing the capacity curve: **a** the building model under a set of horizontal forces and inelastic displacement profiles as the loading increases; **b** the equivalent SDOF system; **c** pushover curve; **d** capacity curve.

subsystem (Garcia et al. 2010). Further than that, it should be noticed that as the wall sub-system is composed by purely flexural members, their flexural strength lies mainly on their capacity to undertake the overturning moment $V_{dw}H_e$, where H_e represents the effective (modal) height of the equivalent SDOF system. This height may be determined as the effective modal height using the mode vector Φ (e.g. Priestley et al. 2007; Priestley 2000), i.e.:

$$H_e = \Phi^{\mathrm{T}}\mathbf{Mh}/\Phi^{\mathrm{T}}\mathbf{M1} \tag{2f}$$

where h is the vector of the heights of the floor masses from the level of excitement. However, a further simplification can be made taking into account that cantilever (building) systems analyzed by the approximate method of the continuous medium have shown that the first mode effective height varies from $0.726H$ for purely flexural systems, to $0.636H$ for purely shear-type systems (Chopra 2008; Clough and Penzien 1993). It is therefore appropriate, in common types of wall-frame buildings, to assume that H_e may be taken, with reasonable accuracy, equal to 2/3 of the total height.

2.1 Assigning Strength and Rigidity to the Frame Sub-system

Let's assume that the shear force sustained by the particular f-frame is equal to V_f, where $\Sigma V_f = V_{df}$, and that the i-column resists a shear force equal to V_i ($\Sigma V_i = V_f$). Prior to an assignment of strength in the frame members it is worth demonstrating the relation among deflections, rigidities and strength. Envisaging the beam-column sub-assemblage of Fig. 2a, with half story heights above and below the joint and half beam lengths on either side of it, and the bending moment diagrams on each member, the elastic inter-story drift of a frame with story heights equal to h, when the joint centre is restrained against rotation, is equal to (Fig. 2b):

$$\theta_c = \frac{V_i h}{6(EI_{co}/h + EI_{cu}/h)} \tag{3a}$$

In the expression above, EI_{co}, EI_{cu} are the rigidities of the column sections, above and below the joint under consideration, which are still unknown. In the case that $I_{co} = I_{cu} = I_c$ and taking into account the diaphragmatic action of the floor slabs (that is, taking θ_c to be the same for all columns), the equation above takes the form

$$\theta_c = \frac{V_i h}{12EI_c/h} = \frac{\Sigma(V_i h)}{12\Sigma(EI_c/h)} = \frac{V_f h}{12\Sigma(EI_c/h)} \tag{3b}$$

Because of the beam flexure, the joint rotation adds an inter-story drift (Fig. 2b) equal to

$$\theta_b = \frac{V_i h}{6(EI_1/l_1 + EI_2/l_2)} \tag{3c}$$

where EI_1, EI_2 and l_1, l_2 are the rigidities and lengths of the beams shown in Fig. 2a. Assuming that θ_b is the same for all joints, and expressing the beam rigidity with the general term EI_b and its length as l_b, the equation above gives:

$$\theta_b = \frac{\Sigma(V_i h)}{12\Sigma(EI_i/l_i)} = \frac{V_f h}{12\Sigma(EI_b/l_b)} \tag{3d}$$

The total elastic drift, for an elastic frame, therefore is

$$\theta_f = \theta_b + \theta_c = \frac{V_f h}{12}\left[\frac{1}{\Sigma(EI_b/l_b)} + \frac{1}{\Sigma(EI_c/h)}\right] \tag{4}$$

For buildings designed according to the strong column - weak beam concept, the yield drift corresponds to the condition that the beam elements yield at their ends. Under the assumption that the frame shear V_f is constant all over the height of the frame, and assuming further that equal yield moments are formed at the ends of all beams at any story, that is (with reference to Fig. 2a) assuming that

$$M_{b1} = M_{b2} = \ldots M_{by} \tag{5}$$

then, the sum of beam yielding moments, at the ends of all beams in any story, will be equal to

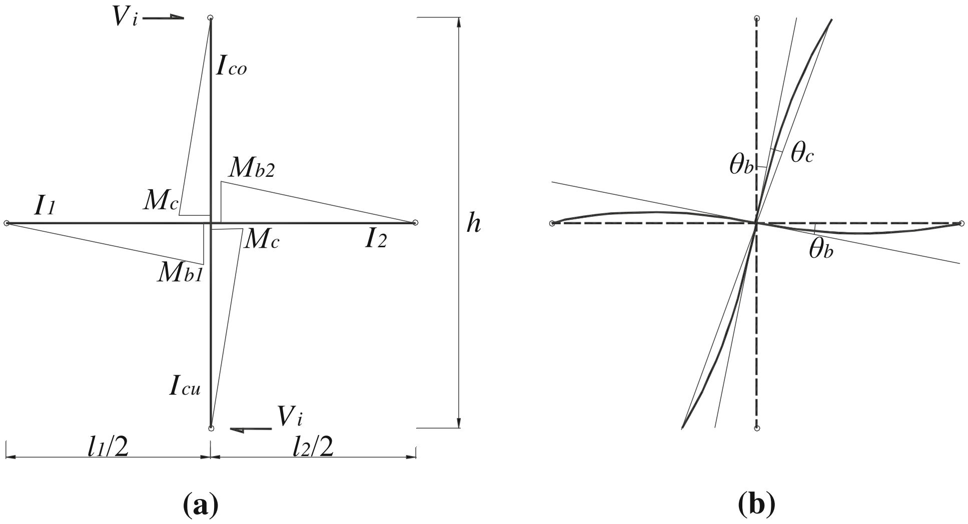

Fig. 2 **a** Typical beam-column frame sub-assemblage; **b** drift components due to column flexure and joint rotation.

$$\Sigma M_{by} = V_f h \tag{6a}$$

For a frame with N columns, the first part of Eq. (6a), is equal to $2(N-1)M_{by}$, and therefore the equation above specifies the beam yield moments as

$$M_{by} = \frac{V_f h}{2(N-1)} \tag{6b}$$

Note here that in practice positive and negative bending moment capacities are not necessarily equal in concrete sections, depending mainly on the magnitude of the gravity loads and also on the tensile reinforcement into the effective slab width affecting the hogging (negative) moment capacity. However, using moment redistribution rules, it is quite possible to end up with positive and negative moments close to each other. Further than that, for ductility reasons, the code suggestions are to provide compression reinforcement exceeding half of the tensile reinforcement, bringing closer the two capacities and this is particularly notable in advanced post elastic stages, due to the deep compression zone for negative moments and strain hardening for positive (sagging) moments (Priestley 1996). In any case, the moments of Eq. (6b) may be taken as the mean values of the two bending capacities and can be used to determine the flexural rigidities of beams and columns in Eq. (4), in combination with Eq. (1a) and (1c). That is: for any beam whose moment–curvature diagram is idealized by the dash bilinear curve of Fig. 3a, its effective rigidity is equal to

$$(EI)_{be} = \frac{M_{by}}{\Phi_{by}} = \frac{M_{by}}{k_b \varepsilon_y} d_b \tag{7a}$$

which means that, for computational purposes, the beam effective second moment of area can be determined as

$$I_{be} = \frac{(EI)_{be}}{E_c I_{bg}} I_{bg} = a_{be} I_{bg} \tag{7b}$$

where E_c is the concrete modulus of elasticity and I_{bg} is the second moment of area of the gross concrete section about the centroidal axis ignoring the reinforcement. Similarly, from the equilibrium of moments around the joint of Fig. 2a, and taking into account that column yield is prevented, the average column moment (the mean value of the moments above and below the joint in the case that the points of contraflexure in the two stories are not at the mid height) will be equal to

$$M_c = M_{by} \tag{8}$$

As columns remain into the elastic stage, the above M_c column moments are fractions of their yield values and if the corresponding curvatures are defined as Φ_c, the slope M_c/Φ_c is higher than the column flexural rigidity, defined as M_{cy}/Φ_{cy}. This is because the bilinear shape of column moment–curvature relationship, shown in Fig. 3b by the dotted line, is an approximate shape, based mainly on the bending moment capacity of the column. Neglecting the effect of the axial load on the column bending capacity and magnifying its value by a factor of 1.25 to ensure that column yielding is prevented (i.e., $M_{cy} = 1.25M_{by}$) and assuming further that $\Phi'_c = 0.8\Phi_{cy}$ (Fig. 3b) the column stiffness can be estimated by the following expression

$$(EI)_{ce} = \frac{M_c}{\Phi_c} = \frac{M_{cy}}{\Phi'_c} \approx 1.5\frac{M_{by}}{\Phi_{cy}} = 1.5\frac{M_{by}}{k_c \varepsilon_y} d_c \tag{9a}$$

As for the case of beams, for computational purposes, the column effective second moment of area may be taken as

$$I_{ce} = \frac{(EI)_{ce}}{E_c I_{cg}} I_{cg} = a_{ce} I_{cg} \tag{9b}$$

Evidently, in exterior beam-column joints the column moment will be equal to half of that of Eq. (8) and therefore the stiffness of edge columns will be half of that given by

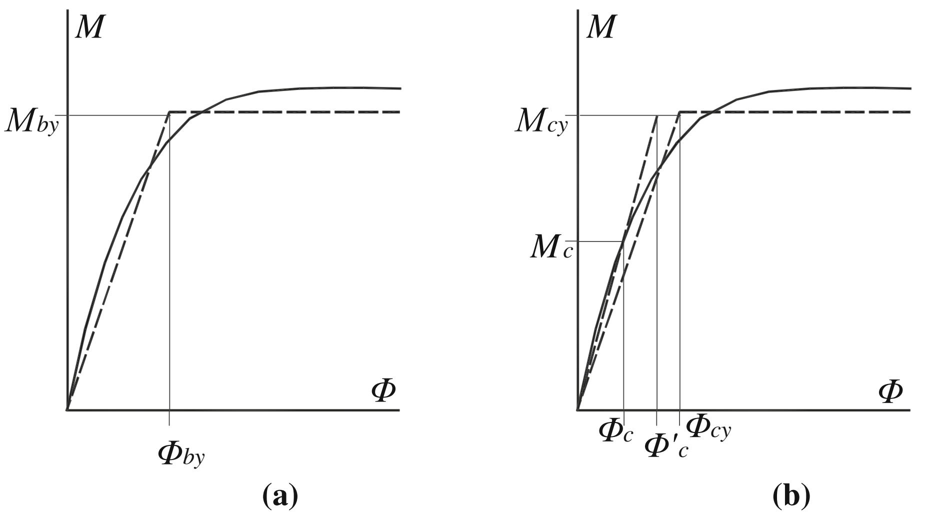

Fig. 3 Typical moment–curvature diagrams of **a** beams and **b** columns of R.C. elements.

Eq. (9a). Note here that induced axial compression loads in column sections affect their flexural strengths (typical bending moment-axial load (M–N) interaction diagrams indicate this relationship). When the axial load is below the 'balance point' of the mentioned diagrams, the column bending moment capacity assessed by Eq. (8) is underestimating the true column capacity, but this assessment does not really affect the yield drift of the frame as explained further below.

Buildings designed according to the capacity design concept (strong column-weak beam model) require further the yield moment at the ground column bases. An estimate of these values can be made by assuming that the point of contraflexure in the first story columns is at a height 0.6*h*. Therefore, if at the top of these columns, the moments developed to maintain equilibrium (around the interior joint of Fig. 2a) are given by Eq. (8), the yield moments at their bases, when a magnifying factor of 1.25 has been taken into account, may be estimated as

$$M_{cy} = (6/5)1.25 M_{by} \tag{10}$$

For edge columns, the base yield moments will be half of those assessed by the equation above.

2.2 Assigning Strength and Rigidity to the Wall Sub-system

Wall elements should be designed to resist an overturning moment equal to $V_{dw}H_e$. Again the designer has the choice to allocate different fractions of this bending moment to the various wall elements: from the classical method, in proportion to the traditionally defined (elastic) stiffness, to the methodology of having the same longitudinal steel ratio in all walls, as proposed by Paulay (1998).

Let's assume that M_w is the bending moment capacity of the particular *w*-Wall, where

$$\Sigma M_w = V_{dw}H_e. \tag{11}$$

Its effective flexural rigidity, in combination with Eq. (1b), will be equal to

$$(EI)_{we} = \frac{M_w}{\Phi_{wy}} = \frac{M_w}{k_w \varepsilon_y} d_w \tag{12a}$$

and the corresponding wall effective second moment of area

$$I_{we} = \frac{(EI)_{we}}{E_c I_{wg}} I_{wg} = a_{we} I_{wg} \tag{12b}$$

Note that axial compression loads sustained by wall sections affect their flexural strengths and, when the mean compression stress reflects a low fraction of the concrete compression strength (as suggested by many building codes), the moment capacity may be higher. As a result the effective second moment of area determined by Eq. (12b) represents a conservative estimate of this property at the base of the wall. In practice however, the reinforcement content is gradually reduced at higher levels, resulting in lower bending capacities and therefore in reduced flexural rigidities. Therefore, for a preliminary structural design, it is considered satisfactory to assess the wall effective second moment of area by means of Eq. (12b).

3. Limits of Inelastic Dispacements

Having defined the beam, column and walls bending moment capacities, as described above and their flexural rigidities by means of Eqs. (7b), (9b) and (12b), the pushover analysis of any planar or symmetrical building system can easily be performed. The inelastic limits of the relative base shear-top deflection curve are dependent partly on the deformation capacities (strains) at the locations of potential plastic hinges and partly on the code drift limits. Concrete sections detailed according to the regulations of modern building codes (with respect to the longitudinal and lateral reinforcement, the concrete strength, the axial load ratio, etc.) may easily possess a plastic rotation capacity of $\theta_p = 0.015$ rads, particularly when, as it is recommended by some codes (e.g. EAK 2000), the ratio of the ultimate to yield curvature, Φ_u/Φ_y, is higher than 10. Under these circumstances, probably the key limit for the pushover curve is the allowable drift. According to EC8 2004 (clause 4.4.3.2), the inter-storey drift is limited to 1.25% for buildings with non-structural elements, to 1.87% for buildings having ductile non-structural elements and, to 2.5% for buildings without non-structural elements. In buildings designed to undergo a beam-sway mechanism, the plastic story drift is directly related to the plastic rotational capacity of beams. For example, when a plastic rotation equal to θ_p is developed in a beam plastic hinge, formed adjacent to the beam-column joint, the story drift is equal to

$$\theta_m = \theta_y + \theta_p \tag{13a}$$

where θ_y is the yield story drift, which may be assessed from the considerations outlined in the previous sections. That is, inserting Eqs. (7a) and (9a) into Eq. (4), the yield drift of the frame is equal to

$$\theta_{fy} = \frac{V_f h \varepsilon_y}{12 M_{by}} \left[\frac{k_b}{\Sigma(d_b/l_b)} + \frac{k_c}{1.5\Sigma(d_c/h)} \right] \tag{13b}$$

For equally spaced columns of the same section, the equation above takes the form

$$\theta_{fy} = \frac{\varepsilon_y}{6} \left[\frac{k_b}{(d_b/l_b)} + \frac{k_c}{1.5(d_c/h)} \right] \tag{13c}$$

which is similar to that given by Aschheim (2002) for regular steel moment-resistant frames. It is also interesting to note that for common types of R.C. frames, under the assumption that the coefficient k_b of Eq. (1c) is increased by 35% to account to joint shear deformations and beam bar slip (Priestley 1998) and assuming a steel yield strain $\varepsilon_y = 0.002$, the formula above provides a more or less constant value of yield drift of the order of 1%. It is evident that for a such yield drift, the beam plastic rotation capacity θ_p of 0.015 rads is hardly attained, because of the code restrictions on the maximum story drifts. It should be mentioned here that first yielding should be expected in walls, not in frames. As noticed in the previous section, the wall sub-system (and the associated element in the equivalent SDOF system) is a purely flexural system and an estimate of its yielding displacement, at the height H_e, can be calculated by using the curvature of Eq. (1b), which is practically independent of the flexural strength of the wall members, i.e.:

$$\Delta_{wy} = \frac{\Phi_{wy} H_e^2}{3} \tag{14a}$$

while, for the frame sub-system, which is a purely shear-type system, the yield displacement at the height of the equivalent SDOF system, will be equal to

$$\Delta_{fy} = \theta_y H_e \tag{14b}$$

The displacement ratio

$$\frac{\Delta_{wy}}{\Delta_{fy}} = \frac{2}{9} \frac{k_w \varepsilon_y}{\theta_y} \left(\frac{H}{d_w} \right) \tag{14c}$$

for $k_w = 1.8$, $\varepsilon_y = 0.002$, $\theta_y = 0.01$ and d_w/H into the practical range from 0.10 to 0.18, takes values between 0.8 and 0.44, indicating that the onset of yielding is expected in the wall elements (Paulay 2001). However, in the case of frames which sustain rather large beam gravity loads, (gravity-dominated frames) first yielding may appear at the edges of beams, particularly when the ratio above attains values close to unity.

4. The Fundamental Frequncy by the Continuous Approach and Estimates of the Reduction Factor and Ductility Demand

For uniform over the height buildings, responding in a translational mode, estimates of the first mode dynamic data (frequency, effective mass, yield displacement) can be made by means of the approximate continuous approach, where the structure is treated as a continuous medium. As follows, the evaluation of these quantities can be implemented by hand calculations without the need to perform any structural analysis. It is therefore useful for the preliminary stage of a practical application. Note that the following formulation is based on the grounds that the flexural rigidities (as calculated in Sect. 2) are 'compatible' with the concept of the beam-sway mechanism and further below, in the numerical example of Sect. 6, the results of this analysis are compared with the corresponding values derived from the capacity curve of the equivalent SDOF system. It is reminded here that the first objective of the paper is to examine whether the first mode dynamic characteristics of the structure, with the aforesaid rigidities, are close to the 'elastic' characteristics of the equivalent SDOF system (frequency and yield displacement or yield acceleration).

The yield shear stiffness of the f-frame is equal to

$$GA_{fy} = V_f / \theta_{fy} \tag{15a}$$

and the total shear stiffness of the frame sub-system is equal to the sum of the above frame stiffnesses. Taking into account that the variation of yield drifts, as expressed by Eq. (13c), is very small for a given steel yield strain, the overall shear stiffness may be approximated by the formula

$$GA_{ty} = \Sigma GA_{fy} = \Sigma V_f / \theta_y = V_{df} / \theta_y = \lambda V_d / \theta_y \tag{15b}$$

where θ_y may be taken as the average value of the frame yield drifts.

Similarly, as the total flexural rigidity of the wall sub-system is given by the sum of the rigidities of Eq. (12a), for walls having the same depth (d_w), the total rigidity will be equal to

$$\begin{aligned}(EI)_{te} &= \Sigma (EI)_{we} = \frac{\Sigma M_w}{\Phi_{wy}} = \frac{V_{dw} H_e}{k_w \varepsilon_y} d_w = \frac{(1-\lambda) V_d H_e}{k_w \varepsilon_y} d_w \\ &= \frac{2}{3} \frac{(1-\lambda) V_d H}{k_w \varepsilon_y} d_w \end{aligned} \tag{15c}$$

Given the total shear and bending stiffness (Eq. (15b) and (15c)), the first mode frequency of any planar (or symmetrical) structure may be determined by the approximate formula (Heidebrecht and Smith 1973; Heidebrecht 1975; Georgoussis 2008):

$$\begin{aligned}\omega^2 &= 1.875^4 \left[1 + \frac{(\alpha H)^2}{1.875^2} \right] \frac{(EI)_{te}}{\bar{m} H^4} \\ &= 1.875^4 \left[\frac{1}{(\alpha H)^2} + \frac{1}{1.875^2} \right] \frac{GA_{ty}}{M_{\mathrm{tot}} H} \end{aligned} \tag{15d}$$

where $\bar{m}$ is the mass per unit height, M_{tot} is the total mass ($= \bar{m} H$) and

$$\alpha H = \sqrt{\frac{GA_{ty}}{(EI)_{te}}} H = \sqrt{\frac{3}{2} \frac{\lambda}{(1-\lambda)} \frac{k_w \varepsilon_y}{\theta_y} \frac{H}{d_w}} \tag{15e}$$

For the practical range of λ from 0.3 to 0.4, and d_w/H from 0.10 to 0.18, the parameter αH varies from 1.1 to 1.9, when $k_w = 1.8$, $\theta_y = 1\%$ and $\varepsilon_y = 0.002$. For such values of αH the variation of the corresponding first mode effective mass, M_e^*, is very narrow [between 0.623 and 0.645 of the total mass (Georgoussis 2014)] and therefore it can be taken approximately equal to $0.635 M_{tot}$.

Equation (15d), in combination with Eq. (2a) takes the form

$$\omega^2 = 1.875^4 \left[\frac{1}{(\alpha H)^2} + \frac{1}{1.875^2} \right] \frac{\lambda \beta}{\theta_y H} g \tag{16a}$$

and the yield displacement of the equivalent SDOF system is equal to

$$u_y = \frac{V_d}{M_e^* \omega^2} = \frac{\beta}{0.635} \frac{g}{\omega^2} \tag{16b}$$

It is evident that for preselected values of β and λ, the evaluation of the period of the structure (through Eq. 16a) is a straightforward procedure and therefore the determination of the expected peak acceleration, A, of the system (through the design (elastic) acceleration spectrum and a predefined damping coefficient). As the yield acceleration of the equivalent SDOF system is given as

$$A_y = u_y \omega^2 = \frac{V_d}{M_e^*} = \frac{\beta}{0.635} g \tag{16c}$$

the corresponding reduction factor is equal to

$$R = A / A_y \tag{17}$$

and the required ductility, μ, can be estimated from any of the methodologies found in the literature for constructing inelastic spectra. Qualitative reviews are presented by Chopra and Goel (1999, 2000) and comparisons are made with the classical method of Newmark and Hall (described in Chopra 2008), where the criterion of equal displacement or equal energy, depending on whether the period of the system falls into the acceleration or velocity sensitive region, is used to relate R and μ. Alternatively, the acceleration–displacement (A–D) demand diagrams can be used as described by Fajfar (2000). In any case, the required (demand) inelastic displacement μu_y should be less than the maximum displacement, u_m, of the capacity curve. The evaluation of the later quantity requires a pushover analysis to be performed on the discrete multi-story building and cannot be assessed by considerations on linear systems.

5. Structural Configurations for Optimum Torsional Responce

The square value of the fundamental frequency of a symmetrical system, given by Eq. (15d), may also be assessed by the sum of the square values of the element frequencies, each of which is defined as the frequency of a particular bent when it is assumed to carry the complete mass of the building. This is Southwell's formula (Newmark and Rosenblueth 1971), expressed as

$$\omega^2 \approx \Sigma \omega_f^2 + \Sigma \omega_w^2 \tag{18}$$

where for the f-Frame and w-Wall, the corresponding element frequencies are respectively equal to

$$\omega_f^2 = \frac{\pi^2}{4} \frac{GA_{fy}}{\bar{m} H^2}, \; \omega_w^2 = 1.875^4 \frac{(EI)_{we}}{\bar{m} H^4} \tag{19}$$

In the case of structures composed by very dissimilar bents (e.g. walls and frames), a higher accuracy in predicting the frequency ω, can be attained with the use of the effective element frequencies, given as (Georgoussis 2014):

$$\bar{\omega}_f^2 = \frac{\pi^2}{4} \frac{GA_{fy}}{\bar{m} H^2} \frac{M_{ef}^*}{M_e^*}, \; \bar{\omega}_w^2 = 1.875^4 \frac{(EI)_{we}}{\bar{m} H^4} \frac{M_{ew}^*}{M_e^*} \tag{20}$$

where M_{ef}^* and M_{ew}^* are respectively the first mode effective masses of the f-Frame and w-Wall, which, when analyzed by the approximate method of the continuous medium, are found equal to $0.81 M_{tot}$ and $0.613 M_{tot}$ (Chopra 2008; Clough and Penzien 1993; Georgoussis 2014). As outlined in recent author's papers (Georgoussis 2008, 2009, 2010, 2012, 2014, 2015), basic dynamic properties of low or medium height uniform buildings may be determined from the analysis of two simpler systems: (i) the corresponding uncoupled multi-story structure which provides the first mode frequency, ω, and the effective mass, M_e^*, and, (ii) a torsionally coupled equivalent single story system, which has a mass equal to M_e^*, radius of gyration equal to that of the typical floor, and it is supported by elements with stiffnesses equal to the product of M_e^* with the squared effective element frequencies ($\bar{\omega}_f^2$ or $\bar{\omega}_w^2$). Therefore the later quantities may be seen as the relative stiffnesses of the elements which provide the lateral resistance of the equivalent single story system. Its analysis, in the linear phase, is very simple and can be found in many past papers (e.g. Georgoussis 2009, 2010), but the main point is that when center of stiffness of the equivalent single story system (m-CR) lies on (or within a close distance from) the mass axis, the torsional response of the real building is mitigated. The distance of m-CR from the center of mass (CM) of the equivalent single story system, along, say, the principal x-axis in a coordinate system with the origin at CM, is equal to

$$x_{m-CR} = \frac{\Sigma(x_w \bar{\omega}_w^2 + x_f \bar{\omega}_f^2)}{\Sigma(\bar{\omega}_w^2 + \bar{\omega}_f^2)} \tag{21}$$

where x_w, x_f are respectively the distances of the w-Wall and f-Frame from CM. Note here that the denominator of Eq. (21) is given from Eq. (18) and a rapid estimate of $\bar{\omega}_f^2$ or $\bar{\omega}_w^2$ may be obtained under the following conditions.

In dual systems, in which all frames are the same, or the variation of yield drifts, as expressed by Eq. (13c), is very small and equal design forces have been assigned to them, the effective element frequencies will be practically equal to each other and their sum will be equal to

$$\Sigma \bar{\omega}_f^2 = \frac{\pi^2}{4} \frac{GA_{ty}}{\bar{m} H^2} \frac{M_{ef}^*}{M_e^*} \tag{22a}$$

Similarly, for walls having the same depth (d_w) and designed to sustain equal shear forces, their effective element frequencies will also be equal to each other, and their sum equal to

$$\Sigma \bar{\omega}_w^2 = 1.875^4 \frac{(EI)_{te}}{\bar{m} H^4} \frac{M_{ew}^*}{M_e^*} \tag{22b}$$

Under these conditions, the ratio

$$\frac{\Sigma\bar{\omega}_f^2}{\Sigma\bar{\omega}_w^2} = \frac{\pi^2}{4 \times 1.875^4}(aH)^2 \frac{0.81}{0.613} \tag{22c}$$

depends only on the parameter αH, and this provides a rapid assessment of $\bar{\omega}_f^2$ or $\bar{\omega}_w^2$, as their sum is already known from Eq. (18). As a result the location of m-CR, is readily computed and, obviously when $x_{m\text{-}CR}$ is equal to zero, the response of the building in the elastic phase is expected to be practically translational. This is investigated in the numerical example which follows.

6. Numerical Example

To illustrate the seismic response of a medium height R.C. dual building, which has been detailed as outlined above, the ten story mono-symmetric concrete building, shown in Fig. 4a is analyzed under the ground motion of Kobe 1995, component KJM000. The building is uniform over the height, with an orthogonal floor plan of 25 × 15 m and the symmetrical counterpart structure is shown in Fig. 4b. The total mass per floor is m = 305.8 kNs^2/m (assuming a total gravity load density of 8 kN/m^2), uniformly distributed over the floor slab, the radius of gyration about CM is r = 8.416 m, the story height is 3.5 m and the concrete modulus of elasticity is assumed equal to 30 × 10^6 kN/m^2, typical for concrete structures. The lateral resistance along the y-direction is provided with six resisting elements, two of which are flexural shear walls (Wa, Wb) with a cross section of 40 × 500 cm and, also, by four moment resisting frames (FR) composed by three columns of dimensions 60 × 60 cm, 6 m apart, which are connected by floor beams 30 × 60 cm. The lateral resistance along the x-axis is provided by a pair of flexural shear walls (Wx) of a cross Section 30 × 650 cm, located symmetrically to the axis of symmetry at distances ±6.6 m as shown in Fig. 4a. The analyzed building represents a typical dual system in the y-direction and a wall system in the x-direction. All the aforementioned lateral load resisting elements are assumed to have only in-plane stiffness. To investigate the accuracy of the proposed method in a broader range of building structures, different structural configurations of the example structure are examined as follows: The four moment resisting frames are located at fixed positions, asymmetrically to CM, as shown in the aforementioned figure. The first wall (Wa) is located on the left of CM, at a distance equal to 3 m, while the second wall (Wb) is taking all the possible locations (denoted as x) along the x-axis.

The symmetrical counterpart structure (Fig. 4b) is designed to resist a horizontal force equal to $V_d = \beta W = 0.2\ W$, 9% of which is decided to be sustained by each of the frames (λ = 0.36) and the rest of the horizontal load to be equally resisted by the two walls. At first estimates are made by means of the approximate continuous approach. The yield drift (Eq. 13c), for $k_b = 1.7 \times 1.35$, $k_c = 2.12$ and $\varepsilon_y = 0.002$ is found equal to $\theta_y = 1.04\%$ and, from Eq. (15e), $\alpha H = 1.43$. Therefore, the fundamental frequency of the system (from Eq. (16a) and the associated period) is equal to $\omega = 4.307$/s (T = 1.459 s). Assuming that this frequency represents the frequency of the equivalent SDOF system, its yield acceleration and displacement (from Eq. (16b) and (16c) are respectively equal to

$$u_y = 0.167\ \text{m}, \quad A_y = 0.31\ \text{g} \tag{23}$$

The same quantities are also calculated with the use of the stiffness matrix method by means of the academic software SAP2000-V16. With the design shear being equal to $V_d = \beta W = 0.2\ W = 6000$ kN, the effective second moments of area are found (from Eqs. 7b, 9b, 12b) equal to $I_{be} = 0.381 I_{bg}$, $I_{ce} = 0.328 I_{cg}$ (half of this to edge columns) and $I_{we} = 0.498 I_{wg}$. Using these data and analyzing the building as a linear system, the fundamental frequency of vibration was found equal to $\omega = 4.111$/s (T = 1.528 s) and the corresponding effective modal mass equal to $M_e^* = 0.667 M_{tot}$. Working as above

$$u_y = \frac{V_d}{M_e^* \omega^2} = \frac{\beta}{0.667} \frac{g}{\omega^2} = 0.174\ \text{m} \quad \text{and} \\ A_y = u_y \omega^2 = \frac{V_d}{M_e^*} = \frac{\beta}{0.667} g = 0.30\ g \tag{24}$$

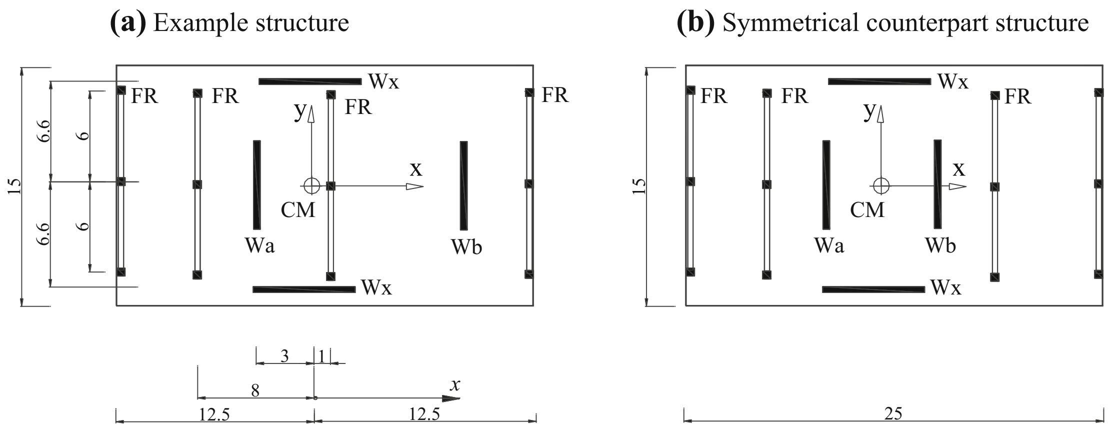

Fig. 4 The example building structure.

To perform the pushover analysis, the required bending moment capacities at the locations of potential plastic hinges (ends of beams, ground column and wall bases) are found from Eqs. (6b), (10) and (11) to be equal to $M_{by} = 472.5$, $M_{cy} = 708.75$ (half at the edge columns) and $M_{wy} = 44800$ kNm. The moment-rotation relationships are assumed bilinear, with a post-yielding stiffness ratio equal to 0.1% and plastic rotation capacity was taken equal to $\theta_p = 0.015$ rads for columns and walls, while for beams an increased capacity, equal to 0.02 rads, was assumed. Using these data and assuming a load shape (vector Φ in Eq. 2) having a linear shape over the height of the building, to simulate a deflection profile of a plastic beam-sway mechanism, the pushover curve thus produced is shown in Fig. 5, together an elasto-plastic approximation, shown by the dotted line. The pushover curve is drawn for three cases of gravity loads: in the first, termed 'Horizontal loading', the gravity loads are neglected, in the second, termed 'Hor+-grav(full)', all the gravity loads of the slab were assumed to be carried by the four frames, which means that each beam of these frames was loaded by a uniformly distributed load of an intensity equal to 62.5 kN/m and, in the last case ('Hor+grav (partial)') the intensity of the beam distributed loading was assumed equal to 2/3 of the previous case. As can be seen, in all cases, first yielding appears at a lateral load (base shear) approximately equal to 5460 kN. Note that in the cases of 'Horizontal loading' and 'Hor+grav (partial)', yielding was initiated at the bases of the wall elements but in the case of 'Hor+grav (full)', the onset of yielding appeared in the beams on the 9th story, a little earlier than yielding in walls. This is an expected response, explained in Sect. 3, that in the case of beams carrying large gravity loads (gravity dominated frames) it is quite possible to have the onset of yielding in beams rather than in walls. As the yield load of 5460 kN is very close to the design load $V_d = \beta W = 6000$ kN, the slope of the initial branch of the approximate elastic–purely plastic curve ('bilinear curve' in Fig. 5) is assumed to coincide with that of the real pushover curves, and its plastic branch is decided to start at a lateral load equal to $V_{do} = 6600$ kN. Envisaging the approximate curve, it may be seen that the above value of V_{do} corresponds to a displacement equal to $\Delta_y = 0.252$ m and that it is adequate to assume that the inelastic displacement capacity reaches the value of $\Delta_m = 0.8$ m. From the latter elasto-plastic pushover curve, in combination with Eq. (2c) and the linear shape of Φ, the frequency, yield acceleration, yield displacement and displacement capacity of the SDOF system are as follows:

$$\omega_e = 3.951/\text{s}\ (T_e = 1.590\ \text{s}), \quad A_y = 0.28\ \text{g}, u_y = 0.176\ \text{m}, \quad u_m = 0.56\ \text{m} \tag{25}$$

By comparison of values shown in the Eqs. (24) and (25), it is evident that the 'initial' characteristics of the equivalent SDOF system (frequency, yield displacement and yield acceleration) are very close to the first mode data of the linear system, when the strength assignment (and the associated flexural rigidities) is 'compatible' with the beam-sway plastic mechanism. The results provided by the approximate continuous approach (Eq. 23), are less accurate, but quite satisfactory for the preliminary stage of a practical application. In all cases, as the period of the structure falls into the velocity sensitive range of commonly used design spectra, the reduction and ductility factors (R and μ) are equal. Note here that the period T_e does not represent a Rayleigh quotient of the first mode period of the linear system, which is found by solving the eigenvalue problem (Chopra 2008).

The response of the eccentric building configurations (defined by the different locations of wall Wb), of Fig. 4a, is investigated under the ground motion of Kobe 1995, component KJM000 (Fig. 6). The structural details are as in the case of the pushover analysis of the symmetrical counterpart structure. The time history analyses were performed using the numerical implicit Wilson-θ time integration method, with the parameter θ taken equal to 1.4 and the damping matrix was assumed stiffness and mass proportional (the damping ratio was taken equal to 5% for the first and third coupled periods of vibration). Note, that minimum torsional response is expected when the location of m-CR coincides with that of CM. That is, when the distance between these points, $x_{m\text{-}CR}$, as given from Eq. (21), is equal to zero. Using the approximate method of the continuous approach, the ratio $\bar{\omega}_f^2 / \bar{\omega}_w^2$, which expresses the ratio of the relative

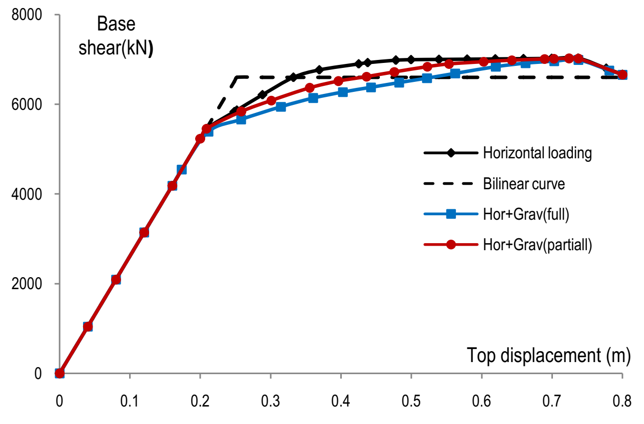

Fig. 5 Pushover curves of the symmetrical counterpart of the example building.

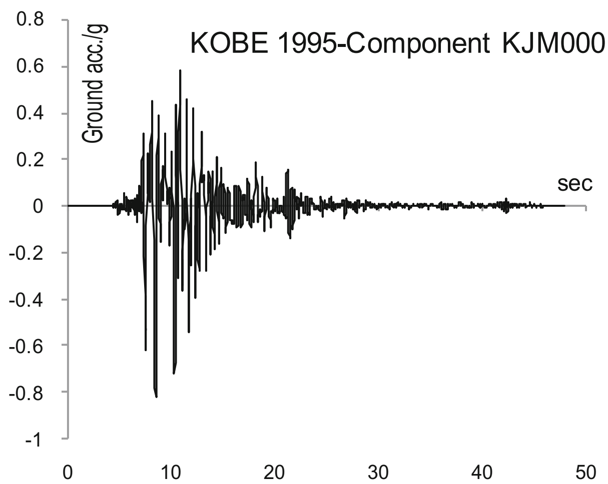

Fig. 6 Ground motion considered.

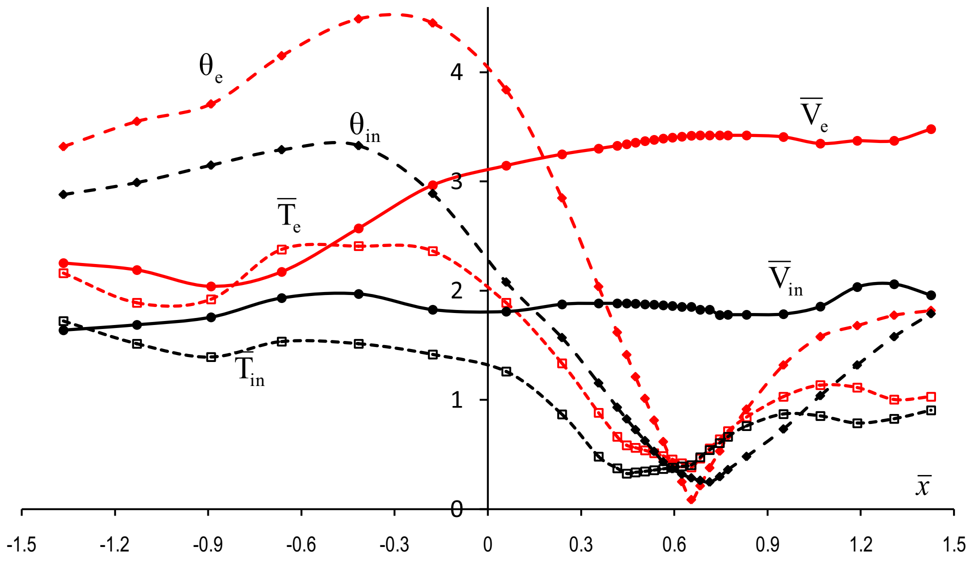

Fig. 7 Top rotations ($\times 10^{-2}$, rads) and normalized base shears and torques of assumed models under the Kobe 1995 ground motion (component KJM000).

stiffnesses of frames and walls (Georgoussis 2014), is equal 0.27, as it is computed from Eq. (22c) and taking into account that four frames and two walls provide the lateral resistance in the y-direction. The same ratio, computed by the stiffness matrix method (SAP2000 software), is found equal to 0.31. Therefore, of all configurations of the structure shown in Fig. 4a, minimum rotation response is expected when the coordinate of Wb is $x = 4.89$ m ($\bar{x} = x/r = 0.58$) or $x = 5.17$ m ($\bar{x} = 0.61$) on the right of CM, depending on the methodology used.

The torsional response of the structural systems of Fig. 4a under the assumed unidirectional (along the y-direction) excitation of Kobe is shown in Fig. 7. Three response parameters are shown for both the elastic and inelastic systems: top rotations, θ, normalized base shears and normalized base torques. The red lines represent the peak elastic response (top rotations: θ_e, are shown by dashed lines, normalized base shears along the y-direction: $\bar{V}_e = V_{ey}/V_d$ by solid lines and normalized base torques: $\bar{T}_e = T_e/rV_d$ by dotted lines) and the corresponding black lines represent the peak response of the inelastic systems (θ_{in}, $\bar{V}_{in} = V_{iny}/V_d, \bar{T}_{in} = T_{in}/rV_d$). Minimum rotational response (in terms of θ_e and $\bar{T}_e$) of the elastic systems appears when the wall Wb approaches the coordinate $\bar{x} = 0.65$, while, at the same location, the level of the elastic normalized shear, $\bar{V}_e$ is a little less of its maximum value. The variation of the base shear of the inelastic systems is quite different. The normalized shear $\bar{V}_{in}$ is almost constant over the full range of locations of wall Wb. The corresponding shear force is approximately equal to 1.85 times the design shear V_d and higher than the shear capacity obtained by the static pushover analysis. This is due to the contribution of the higher modes of vibration and it is explained by Krawinkler and Seneviratna (1998): even in wall structures the higher mode effects amplify the base shears that can be generated in the wall once a plastic hinge has formed at the base. The almost constant value of $\bar{V}_{in}$ may be explained by a finding of Lucchini et al. (2008) that deep into the nonlinear range, the maximum displacements of the different lateral load resisting bents tend to be reached by the same deformed configuration of the system. In other words, in a configuration where all bents deflect in the same direction, deeply into the inelastic phase. The inelastic top rotation, θ_{in}, appears to be minimum at $\bar{x} = 0.71$ and the base torque at $\bar{x} = 0.45$, but the latter is almost constant in the interval of $\bar{x}$ from 0.45 to 0.71. The response of the inelastic systems is smoother and the overall rotational behavior is smaller than that obtained by the elastic behavior. Note here that for locations of wall Wb on the left of CM, increased plastic rotations were sustained by the beams of the frame on the right edge, reaching the value of 0.0175 rads in a location of Wb very close to Wa ($\bar{x} = -0.416$). That is, when the walls Wa and Wb, came very close to each other, their contribution to the torsional stiffness was minimized and the inelastic top rotation, as can be seen in Fig. 7, reached the peak value. This indicates the importance of having structural systems which sustain a limited torsional response. The aforesaid smoother rotational response confirms observations in single story systems that after yielding asymmetric systems have the tendency to deform further in a translational mode (e.g. Ghersi and Rossi 2001). Similar are the results on multistory systems with elements having strength independent stiffnesses (Fajfar et al. 2005; Georgoussis 2014). Regarding the configuration of minimum torsion, it is evident that the predicted one by the condition of having the points m-CR and CM at the same location [$x_{m\text{-}CR} = 0$ in Eq. (21)], is very close to that obtained by 3D dynamic analyses. The fact that at such locations of Wb, the more or less translational elastic response is preserved into the inelastic phase verifies a statement of Lucchini et al. (2009) concerning the behavior of single story buildings: their nonlinear response depends on how the building enters the nonlinear range, which in turn depends on its elastic properties (i.e. the stiffness and mass distributions), and on the capacities of its resisting elements (i.e. the strength distribution).

7. Conclusions

The frequency and the reduction factor, which are the main parameters in the force-based design philosophy of low to medium height buildings, can be evaluated with reasonable accuracy by a simple methodology which (i) allocates strengths in wall-frame dual systems and, (ii) enables the determination of the dependable flexural rigidities in the various structural members. The method can be implemented by both the approximate continuum approach, which is very simple since it is based on a well known formulation and, also, by the stiffness matrix method using a commercial software of structural analysis. This methodology can easily be incorporated in the strategy of constructing structural configurations of minimum rotational response, which is the main requirement in the design of structures expected to sustain strong ground motions. The approach presented is based on simple principles and it is design oriented, useful in the preliminary stage of a practical application, where efficient, practical and economic solutions are sought by the practicing engineer.

Open Access

References

Anagnostopoulos, S. A., Kyrkos, M. T., Papalymperi, A., & Plevri, E. (2015a). Should accidental eccentricity be eliminated from Eurocode 8? *Earthquakes and Structures, 8*(2), 463–484.

Anagnostopoulos, S. A., Kyrkos, M. T., & Stathopoulos, K. G. (2015b). Earthquake induced torsion in buildings: Critical review and state of the art. *Earthquakes and Structures, 8*(2), 305–377.

Aschheim, M. (2002). Seismic design based on the yield displacement. *Earthquake spectra, 18*(4), 581–600.

Aziminejad, A., & Moghadam, A. S. (2009). Performance of asymmetric multistory buildings with different strength distributions. *Journal of Applied Sciences, 9*(6), 1082–1089.

Aziminejad, A., Moghadam, A. S., & Tso, W. K. (2008). A new methodology for designing multi-story asymmetric buildings. In The 14th world conference on earthquake engineering. Oct 14–17, Beijing, China.

Bosco, M., Ferrara, G. A. F., Ghersi, A., Marino, E. M., & Rossi, P. P. (2015). Seismic assessment of existing R.C. framed structures with in-plan irregularity by nonlinear static methods. *Earthquakes and Structures, 8*(2), 401–422.

Chandler, A. M., Duan, X. N., & Rutenberg, A. (1996). Seismic torsional response: Assumptions, controversies and research progress. *European Earthquake Engineering., 1*, 37–51.

Chopra, A. K. (2008). *Dynamics of Structures* (3rd ed.). Upper Saddle River, NJ: Prentice Hall.

Chopra, A. K., & Goel, R. K. (1999). Capacity-demand-diagram methods based on inelastic design spectrum. *Earthquake Spectra, 15*(4), 637–657.

Chopra, A. K., & Goel, R. K. (2000). Evaluation of NSP to estimate seismic deformation: SDF systems. *Journal of Structural Engineering ASCE, 126*(4), 482–490.

Clough, R. W., & Penzien, J. (1993). *Dynamics of structures* (2nd ed.). New York, NY: McGraw-Hill.

De Stefano, M., & Pintucchi, B. (2008). A review of research on seismic behaviour of irregular building structures since 2002. *Bulletin of Earthquake Engineering, 6*, 285–308.

De Stefano, M., Tanganelli, M., & Viti, S. (2015). Seismic performance sensitivity to concrete strength variability: A case-study. *Earthquakes and Structures, 9*(2), 321–337.

EAK. (2000). *Greek aseismic code*. Greece: Greek Ministry of Environment, City Planning and Public Works. (in Greek).

Eurocode 8 (EC8). (2004). Design provisions for earthquake resistance of structures. European Standard EN/1998: 2004

Fajfar, P. (2000). A nonlinear analysis method for performance based seismic design. *Earthquake Spectra, 16*(3), 573–592.

Fajfar, P., Marusic, D., & Perus, I. (2005). Torsional effects in the pushover-based seismic analysis of buildings. *Journal of Earthquake Engineering, 9*(6), 831–854.

Garcia, R., Sullivan, T. J., & Corte, G. D. (2010). Development of a displacement-based design method for steel-RC wall buildings. *Journal of Earthquake Engineering, 14*(2), 252–277.

Georgoussis, G. K. (2008). Optimum design of multistory uniform structures with simple eccentricity. *The Structural Design of Tall and Special Buildings, 17*(3), 719–738.

Georgoussis, G. K. (2009). An alternative approach for assessing eccentricities in asymmetric multistory structures, 1: Elastic Systems. *The Structural Design of Tall and Special Buildings, 18*(2), 181–202.

Georgoussis, G. K. (2010). Modal rigidity center: Its use for assessing elastic torsion asymmetric buildings. *Earthquake and Structures, 1*(2), 163–175.

Georgoussis, G. K. (2012). Seismic analysis of non-proportionate eccentric buildings. *Advanced Material Research, 450–451*, 1482–1488.

Georgoussis, G. K. (2014). Modified seismic analysis of multistory asymmetric elastic buildings and suggestions for minimizing the rotational response. *Earthquake and Structures, 7*(1), 039–52.

Georgoussis, G. K. (2015). Minimizing the torsional response of inelastic multistory buildings with simple eccentricity. *Canadian Journal of Civil Engineering, 42*(11), 966–969.

Ghersi, A., & Rossi, pp. (2001). Influence of bi-directional ground motions on the inelastic response of one-story in-plan irregular systems. *Engineering Structures, 23*, 579–591.

Heidebrecht, A. C. (1975). Dynamic analysis of asymmetric wall- frame buildings. ASCE, National structural engineering convention.

Heidebrecht, A. C., & Smith, B. S. (1973). Approximate analysis of tall wall-frame structures. *Journal of the Structural Division ASCE, 2*, 169–183.

Heo, Y. A., & Kunnath, S. K. (2013). Damage-Based seismic performance evaluation of reinforced concrete frames. *International Journal of Concrete Structures and Materials, 7*(3), 175–182.

Humar, J. L., & Rahgozar, M. A. (1996). Concept of over strength in seismic design. In 11th world conference on earthquake engineering. Acapulco, Mexico, June 23–28

Krawinkler, H., & Seneviratna, G. D. P. K. (1998). Pushover analysis for seismic performance evaluation. *Engineering structures, 20*(4–6), 452–464.

Kyrkos, M. T., & Anagnostopoulos, S. A. (2011a). An assessment of code designed, torsionally stiff, asymmetric steel buildings under strong earthquake excitations. *Earthquake and Structures, 2*(2), 109–126.

Kyrkos, M. T., & Anagnostopoulos, S. A. (2011b). Improved earthquake resistant design of torsionally stiff asymmetric steel buildings. *Earthquake and Structures, 2*(2), 127–147.

Kyrkos, M. T., & Anagnostopoulos, S. A. (2013). Improved earthquake resistant design of eccentric buildings. *Soil Dynamics and Earthquake Engineering., 47*, 144–156.

Lucchini, A., Monti, D., & Kunnath, S. (2008). A simplified pushover method for evaluating the seismic demand in asymmetric-plan multi-story buildings. In The 14th world conference on earthquake engineering, Oct 14–17, Beijing.

Lucchini, A., Monti, D., & Kunnath, S. (2009). Seismic behavior of single-story asymmetric-plan buildings under uniaxial excitation. *Earthquake Engineering and Structural Dynamics, 38*, 1053–1070.

Moghadam, A. S., & Tso, W. K. (2000). 3-D pushover analysis for damage assessment of buildings. *Journal of Seismology and Earthquake Engineering, 2*(3), 23–31.

Newmark, N. M., & Rosenblueth, E. (1971). *Fundamentals of earthquake engineering*. Upper Saddle River, NJ: Prentice-Hall.

Park, R., & Paulay, T. (1975). *Reinforced concrete structures*. Hoboken, NJ: Wiley.

Paulay, T. (1998). A mechanism-based design strategy for the torsional seismic response of ductile buildings. *European Earthquake Engineering, 2*, 33–48.

Paulay, T. (2001). Some design principles relevant to torsional phenomena in ductile buildings. *Journal of Earthquake Engineering, 5*(3), 271–308.

Paulay, T. (2002). An estimation of displacement limits for ductile systems. *Earthquake Engineering and Structural Dynamics, 31*, 583–599.

Paulay, T. (2003). Seismic displacement capacity of ductile reinforced concrete building systems. *Bulletin of the New Zealand Society for Earthquake Engineering., 36*(1), 47–65.

Paulay, T., & Priestley, M. J. N. (1992). *Seismic design of reinforced and masonry buildings*. Hoboken, NJ: Wiley.

Priestley, M. J. N. (1996). Displacement-based seismic assessment of existing RC buildings. *Bulletin of the New Zealand National Society for Earthquake Engineering, 29*(4), 256–272.

Priestley, M. J. N. (1998). Brief comments on elastic flexibility of RC frames and significance to seismic design. *Bulletin of the New Zealand National Society for Earthquake Engineering, 31*(4), 246–259.

Priestley, M. J. N. (2000). Performance based seismic design. 12 WCEE, Auckland, New Zealand.

Priestley, M. J. N., Calvi, G. M., & Kowalsky, M. J. (2007). *Direct displacement based design of buildings*. Pavia, Italy: IUSS Press.

Priestley, M. J. N., & Kowalsky, M. J. (1998). Aspects of drift and ductility capacity of rectangular walls. *Bulletin of the New Zealand National Society for Earthquake Engineering, 31*(2), 73–85.

Rutenberg, A. (1998). EAEE Task Group (TG)8: Behaviour of irregular and complex structures- State of the art report: Seismic nonlinear response of code-designed asymmetric structures. In 11th European conference on earthquake engineering. Rotterdam, Netherlands: Balkema